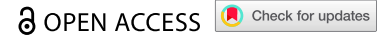



ORIGINAL RESEARCH



BCG-activation of leukocytes is sufficient for the generation of donor-independent innate anti-tumor NK and $\gamma\delta$ T-cells that can be further expanded *in vitro*

Gloria Estesó^a, María José Felgueres^a, Álvaro F. García-Jiménez^a, Christina Reyburn-Valés^a, Alberto Benguría^b, Enrique Vázquez^b, Hugh T. Reyburn^a, Nacho Aguiló^c, Carlos Martín^{c,d}, Eugenia Puentes^e, Ingrid Murillo^e, Esteban Rodríguez^e, and Mar Valés-Gómez^b 

^aDepartment of Immunology and Oncology, National Centre for Biotechnology, Spanish National Research Council, Madrid, Spain; ^bServicio de Genómica, Centro Nacional de Investigaciones Cardiovasculares (CNIC), Madrid, Spain; ^cGrupo de Genética de Micobacterias, Departamento de Microbiología y Medicina Preventiva, Facultad de Medicina, Universidad de Zaragoza, IIS-Aragon; Zaragoza, Spain and CIBER Enfermedades Respiratorias, Instituto de Salud Carlos III; Madrid, Spain; ^dServicio de Microbiología, Hospital Universitario Miguel Servet, IIS Aragon; Zaragoza, Spain; ^eClinical Research Department y Research & Development Department, Biofabri, Grupo Zendal, O'Porriño, Pontevedra, Spain

ABSTRACT

Bacillus Calmette-Guérin (BCG), the nonpathogenic *Mycobacterium bovis* strain used as tuberculosis vaccine, has been successfully used as treatment for non-muscle invasive bladder cancer for decades, and suggested to potentiate cellular and humoral immune responses. However, the exact mechanism of action is not fully understood. We previously described that BCG mainly activated anti-tumor cytotoxic NK cells with upregulation of CD56 and a CD16⁺ phenotype. Now, we show that stimulation of human peripheral blood mononuclear cells with iBCG, a preparation based on BCG-Moreau, expands oligoclonal $\gamma\delta$ T-cells, with a cytotoxic phenotype, together with anti-tumor CD56^{high} CD16⁺ NK cells. We have used scRNA-seq, flow cytometry, and functional assays to characterize these BCG-activated $\gamma\delta$ T-cells in detail. They had a high IFN γ secretion signature with expression of CD27⁺ and formed conjugates with bladder cancer cells. BCG-activated $\gamma\delta$ T-cells proliferated strongly in response to minimal doses of cytokines and had anti-tumor functions, although not fully based on degranulation. BCG was sufficient to stimulate proliferation of $\gamma\delta$ T-cells when cultured with other PBMC; however, BCG alone did not stimulate expansion of purified $\gamma\delta$ T-cells. The characterization of these non-donor restricted lymphocyte populations, which can be expanded *in vitro*, could provide a new approach to prepare cell-based immunotherapy tools.

ARTICLE HISTORY

Received 07 September 2022
Revised 10 November 2022
Accepted 14 December 2022

KEYWORDS

Cancer immunology; BCG; NK activation; gamma delta T lymphocytes; bladder cancer; immunotherapy

Introduction

The attenuated strain of *Mycobacterium bovis*, Bacillus Calmette-Guérin (BCG), was developed in 1921 as a vaccine against tuberculosis (TB), by passaging the pathogenic strain *in vitro* for 15 years.¹ Since then, BCG has been used as a vaccine for TB and, in the last decades, it has been also the therapy of choice for non-muscle invasive bladder cancer.² The immune responses activated by *Mycobacterium tuberculosis* (Mtb) and BCG have been studied extensively, and a number of benefits have been attributed to BCG vaccination. However, there are still many questions regarding the quality and duration of protection from infection and disease, as well as the mechanism of action of BCG, both as a vaccine and as bladder cancer immunotherapy.³ An extra level of complication arises from the fact that many different sub-strains of BCG were generated during the distribution worldwide of the early BCG cultures generated at the Pasteur Institute,^{4,5} so that not all BCG strains have the same molecular profile, and it is not unreasonable to expect disparities in the interaction of different sub-strains with the host. Indeed, phenotypic differences among BCG sub-strains have been described *in vivo*, both in

terms of attenuation level and protective efficacy against tuberculosis challenge.⁶

Several factors, aside from the existence of different BCG sub-strains, contribute to the controversies on the efficacy of BCG as a TB vaccine, including that the methods used to define TB immunity are not always equivalent, and that the duration of immunity is not clear.⁷ Before 2001, the tuberculin skin test was the preferred parameter to define TB immunity, measuring the delayed-type hypersensitivity (DTH) response 48–72 hours after intradermal injection of tuberculin-purified protein derivative (PPD). However, this parameter does not distinguish between Mtb and BCG exposure.⁸ A more recent extended method, is the interferon- γ release assay (IGRA), which measures effector T-cell responses against either PPD or other antigens, such as early secretory antigenic target-6 (ESAT-6) and culture filtrate protein 10 (CFP-10), present in several mycobacteria, but not in BCG.⁹ It is important to note that the T-cell response does not always correlate with protection from infection and disease, and that evidence for the involvement of the innate immune response after BCG and Mtb exposure is accumulating.³ In fact, CD4 T-cells account for

only a third of the cytokine-expressing lymphocytes in response to *in vitro* BCG stimulation, followed by NK cells, $\gamma\delta$ T-cells and mucosal-associated invariant T-cells (MAIT) cells.¹⁰ Moreover, *in vivo*, latent tuberculosis is associated with enhanced cytotoxic responses, mostly mediated by CD16⁺ NK cells, which are decreased during active disease.¹¹ Previous work from our laboratory characterizing NK cell activation after *in vitro* exposure to BCG revealed the generation of a CD56^{high} CD16⁺ population that proliferated in response to an initial wave of monocyte-derived cytokines released to the culture (referred to as CD56^{high} to avoid confusion with peripheral blood immature CD56^{bright} cells).¹² Further, neonatal BCG vaccination as well as BCG re-vaccination of Mtb-infected adults has been associated with increased frequencies of IFN γ -producing BCG-reactive NK cells that persisted at least 1 year after vaccination.¹³ This could be reminiscent of the new concept of trained immunity, which suggests non-peptide/MHC specific protection to infections through reprogramming of innate immune cells for example, by epigenetic changes in monocytes or HCMV-exposure-related phenotypic changes in NK cells.^{14–16} Together with persistent NK cells, CD3⁺CD56⁺ NKT-like cells were also described in BCG-vaccinated individuals.¹³ In this case, CD1 or other innate T-cell markers were not explored. However, it has been shown that infants vaccinated with BCG generate unconventional CD4[−]CD8[−] [double-negative (DN)] T-cells, together with CD4 T-cells and NK cells, that produced IFN γ .⁷ Although not investigated in that trial, these DN T-cells might be $\gamma\delta$ T-cells, another type of innate lymphocytes responding to pathogen-derived molecules, that express few combinations of rearranged TCRs.^{17–19} In fact, $\gamma\delta$ T-cells can be expanded *in vitro* using mycobacterial products.¹⁸

BCG activation of non-peptide/MHC-mediated innate responses might be responsible for some of the beneficial qualities attributed to BCG, including its role in the elimination of bladder cancer. In fact, we have previously reported the activation of anti-tumor NK cells, with cytotoxic capacity against bladder cancer cell lines, after *in vitro* culture of peripheral blood mononuclear cells (PBMC) with BCG.^{12,20} The activation of NK cells occurred from day 5 in culture and was associated with the release of cytokines such as IL2, IL12, IL23, MIP-1 β , and IFN γ . NK activation and proliferation were accompanied by upregulation of CD56. So, a CD56^{high} population was generated, also expressing CD16 and markers of mature NK populations like CD94 and KIR. Activation markers, such as CD69 (transiently) and CD25 also were observed and a significant increased expression of CD16, KIR, CD57, and CD94 was found. To distinguish these cytokine-activated anti-tumor NK cells from immature CD56^{bright} cells, normally found in low percentages of peripheral blood, we refer to BCG-activated NK cells as CD56^{high}. Unconventional CD56^{high} NK cells with potent anti-tumor responses have also been described after stimulation with IL15,²¹ and activated NK cells have been found in peripheral blood of BCG vaccinated infants,²² while adult vaccination led to NK cells able to secrete pro-inflammatory cytokines.²³

Besides NK cells, other innate immune populations have also been shown to develop anti-tumor responses after mycobacteria exposure, in particular, MAIT and $\gamma\delta$ T-cells. Thus, many efforts are being made to obtain innate effector cells from

peripheral blood to include in new immunotherapy regimes.²⁴ For example, BCG, *M. vaccae*, and *M. obuense* induced $\gamma\delta$ T-cell anti-tumor effector responses, indirectly via a specific subset of circulating DCs (secreting IL12, IL1 β , and TNF α).²⁵ It is well documented that mycobacterial-derived phosphorylated non-peptidic compounds activate potently unconventional lymphocytes.²⁶ In particular, human V γ 9/V δ 2-expressing T-cells respond to isopentenyl pyrophosphates (IPP) produced, among others, by bacteria. These cells require the association of butyrophilin to the phosphoantigen to bind the non-variable region of the TCR.²⁷ Thus, $\gamma\delta$ T-cells are regarded as HLA-independent T-cells.²⁴ However, $\gamma\delta$ T-cells generated in the presence of different stimuli can include subpopulations with either a pro-tumorigenic or effector/memory polarization with different surface markers, cytokine production capacity, and effector functions.^{28–31}

Since not all the ways to stimulate the innate immune response with BCG are understood and because different sub-strains can generate differential protection against tuberculosis,³² we decided to study, at a single cell level, the repertoire of innate lymphocytes generated after incubation of PBMC with BCG *in vitro*. We have used single-cell RNA sequencing (scRNA-seq) to define detailed phenotypes that could help to understand the functional capacities of BCG-activated lymphocytes, and to develop new *in vitro* systems for expansion of the desired anti-tumor population. Here, we have studied in parallel the activation exerted by two preparations of BCG and analyzed in depth their phenotype and functional capacities. We discovered that a population of effector innate NK and $\gamma\delta$ T-cells can be expanded *in vitro* by co-culture of PBMC with BCG, followed by a IL12, IL15, IL21 cytokine combination cocktail in minimal doses and a short stimulation with IL18. The exact composition of the effector population varied depending on the sub-strain of BCG used, but a potent anti-tumor response was generated by these innate lymphocyte cultures.

Methods

For detailed methods, see Supplementary Material.

Cells, BCG sub-strains, and reagents

Bladder cancer cell lines, J82, T24, and RT-112, and the erythroleukemia K562 cell line were previously described.¹²

BCG-Tice (OncoTICE, MSD) and ImunoBCG (iBCG, Biofabri, Spain) aliquots were reconstituted in RPMI 10% DMSO and stored at -80°C . PBMCs from buffy coats of healthy donors were obtained from the Regional Transfusion Center (Madrid). For BCG stimulation, experiments were performed as previously described.¹² For experiments with enriched cultures of $\gamma\delta$ T-cells, the TCR γ/δ + T-cell Isolation Kit human was used (130–092–892, Miltenyi Biotec).

scRNA-seq

For scRNAseq, library pools were sequenced at 650 pM in paired-end reads on a P3 flow cell using NextSeq 2000 (Illumina) at the Genomics Unit of the National Center for

Cardiovascular Research (CNIC, Madrid, Spain). R code related to the main scRNA-seq figures can be found at https://github.com/algarji/BCG_scRNA-seq. scRNA-seq data are available at Gene Expression Omnibus (GEO) (GSE203098)

<https://www.ncbi.nlm.nih.gov/geo/query/acc.cgi?acc=GSE203098>.

Results

BCG-Tice and iBCG stimulate different lymphocyte populations

We described recently that different sub-strains of BCG can stimulate NK cells, upregulating CD56 and leading to anti-tumor functional activities.^{12,20} To explore in detail the lymphocyte activation capacity of two BCG strains with clear differences in certain major antigens, we used two vaccine preparations: BCG-Tice (Oncotice) and BCG-Moreau (imunoBCG, iBCG). PBMC from healthy donors were stimulated for 1 week with BCG and analyzed by flow cytometry. In general, the pattern of size changes and complexity of lymphocytes was similar for both BCG sub-strains, as shown by changes in FSC/SSC (Figure 1a) which parallels the presence of activation markers, such as CD69, CD25 (Supplementary Figure 1A, B). However, while the percentage of activated lymphocytes increased from day 6 in Oncotice-activated PBMC, this population was already visible by day 5 in iBCG-activated cells, suggesting a faster response (Figure 1b). Further, iBCG led to the proliferation of an activated CD3⁺ population, mainly lacking CD4 and CD8, which was phenotyped as a $\gamma\delta$ T-cell population (Figure 1c, d, e), as well as NK cells. In contrast, no significant expansion of $\gamma\delta$ T-cells was observed in Oncotice cultures.

The expansion of CD3⁺ $\gamma\delta$ T-cells induced by co-culture of PBMC with iBCG, consistently occurred, although in different proportions, in a total of 35 experiments, performed with 33 donors (Figure 1f). On average, resting PBMC had 3.1% CD3⁺ $\gamma\delta$ T-cells (ranging between 0.1 and 12.7) while the proportion changed to 5–66% after 7 days in culture with iBCG (average = 18.7%; n = 35). Taking into account the total cell number, an increase between 2 and 179-fold was observed (8-fold increase in average) (Supplementary Figure 1C). The percentage of NK cells obtained in Oncotice-activated PBMC cultures at day 7 was in general slightly higher than with iBCG (Figure 2a, b). Interestingly, both sub-strains produced a clear increase in CD56 expression on NK cells surface, indicating the activation of the NK population. Around one-third of $\gamma\delta$ T-cells also expressed the NK marker CD56, a feature already described for certain subpopulations of these non-conventional T-cells.²⁴ Treatment with BCG slightly increased the percentage of CD4 vs CD8 T lymphocytes cells, but only a very small proportion of $\gamma\delta$ T-cells expressed either CD4 or CD8 (Figure 2c). Clonality of the $\gamma\delta$ T-cell population generated upon iBCG-activation was analyzed sequencing TCR γ and δ chains, according to^{33–35} (See Methods and Supplementary Figure 2), revealing no evidence of clonal expansion, although the majority of TCRs identified used the V γ 9V δ 2 chains (Supplementary Figure 3). Interestingly,

however, several TCR $\gamma\delta$ CDR3 sequences identical to those described as associated with high anti-tumor reactivity or other pathogen infections were found.^{34,35}

Although $\gamma\delta$ T-cells had already been reported to respond to BCG co-incubation, the repertoire of $\gamma\delta$ T-cells activated by different stimuli can express completely different phenotypes and functional capacities.^{36–38} Thus, to understand the anti-tumor immune activity stimulated by BCG and the possibility of expanding immune effector cells that contribute to the elimination of solid tumors, it was necessary to carry out an in-depth characterization of the $\gamma\delta$ T-cells obtained in co-cultures with iBCG and their tumor recognition capacity.

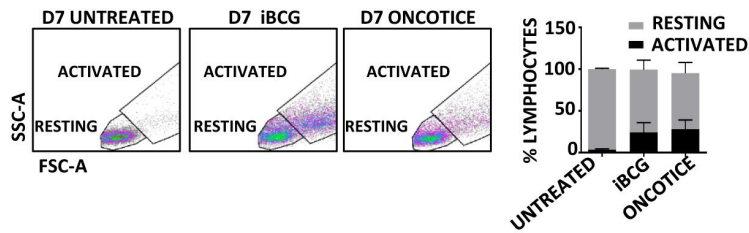
iBCG stimulates the proliferation of activated CD27⁺ IFN γ -producing $\gamma\delta$ T lymphocytes

In order to perform an unbiased characterization of the detailed phenotype of the population of $\gamma\delta$ -CD3⁺ cells and other immune cells activated by BCG, scRNA-seq analyses of iBCG- and Oncotice-stimulated PBMC from three healthy donors were performed.

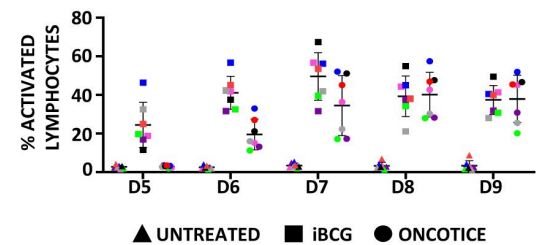
After quality control evaluation (Supplementary Figure 4A, B, C), the transcriptome was analyzed. Clustering analysis followed by two-dimensional *Uniform Manifold Approximation and Projection* (UMAP)³⁹ allowed the definition of 12 distinct clusters (Figure 2d, Supplementary Figure 4D). These clusters were defined on the basis of differential gene expression between all cells, and the markers used for annotation are shown in Figure 2e and Supplementary Figure 5. As observed in our initial flow cytometry experiments, inspection of the transcriptome revealed a $\gamma\delta$ T-cell population clearly expanded in iBCG-activated cells, while NK cells, TEM, and CD4 T-cells expanded more in Oncotice-activated PBMC. Expression of specific NK markers both in scRNA-seq and flow cytometry analyses confirmed a similar NK activation and phenotype (Supplementary Fig. 6, 7). Besides NK and $\gamma\delta$ T-cells, other lymphocyte populations were also identified in BCG-activated cultures by scRNA-seq, including proliferating of CD4 T-cells and CD8 TEM, mainly found in PBMC treated with Oncotice (Figure 2d, e). CD8 TEM had an effector phenotype, as shown by the presence of granzymes, perforin, and the cytotoxicity-related molecules GNLV (granulysin) and FGFBP2 (the secretory protein Ksp37) (Supplementary Figure 7C). A small number of monocytes, B cells, and plasma cells were also identified in our initial analyses (Figure 2d, e).

Pseudobulk analysis showed that PBMC from the three donors stimulated with iBCG had very consistent differential expression of the genes encoding TCR gamma and delta chains, TRDV2 and TRGV9 (Figure 2f). Closer inspection of iBCG-activated cells showed high expression of CD27 (TNFRSF7), a T-cell costimulatory molecule member of the TNF-receptor superfamily that has been described in a subset of IFN γ -producing $\gamma\delta$ T-cells⁴⁰ and related with long-term maintenance of T-cell immunity.⁴¹ Other abundantly expressed genes identified included CCL5 (RANTES), granzymes (GZMK, GZMA), and a number of NK receptors [KLRB1 (CD161), KLRC1 (NKG2A), KLRD1 (CD94), and KLRK1 (NKG2D)]. All these markers, which were

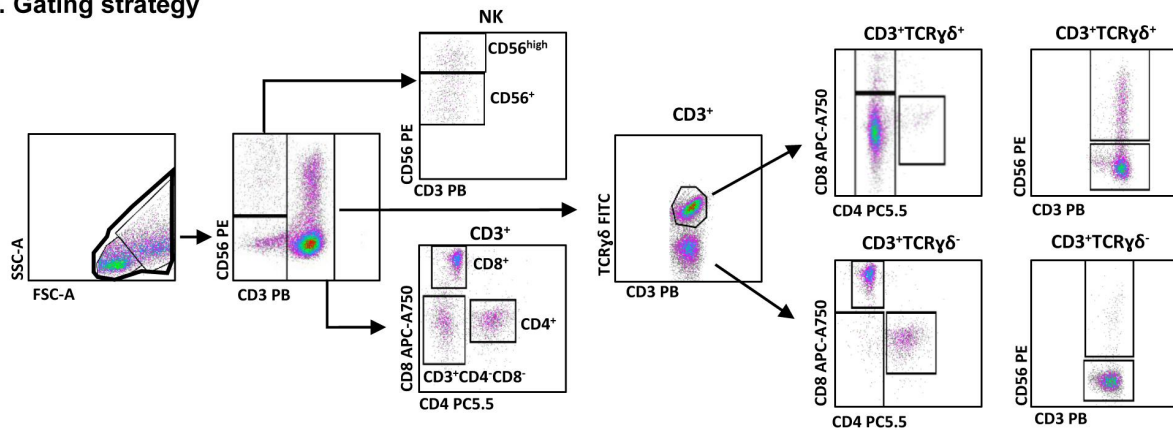
a. BCG PBMC activation



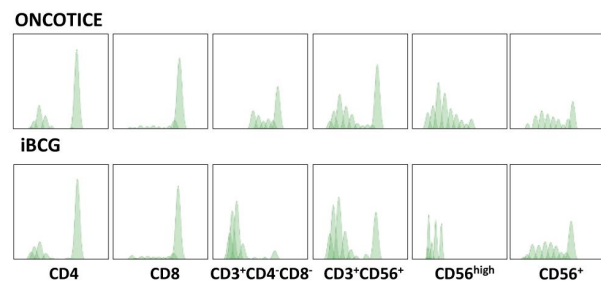
b. BCG lymphocyte activation



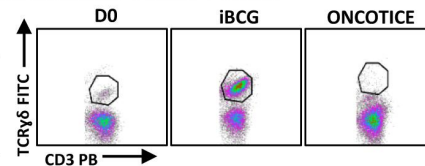
c. Gating strategy



d. Lymphocyte proliferation



e. Gamma-Delta T cells



f.

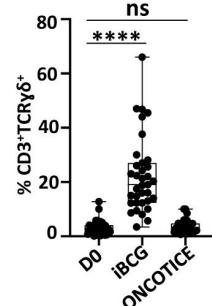


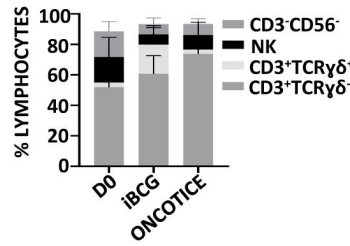
Figure 1. Incubation with iBCG leads to expansion of $\gamma\delta$ T-cells. PBMC from healthy donors were incubated with the sub-strains of BCG iBCG or Oncotice at a 6:1 ratio (total bacteria to PBMC). At the indicated days of culture, cells in suspension were recovered from the co-culture and analyzed by flow cytometry. **a. Lymphocyte activation.** The percentage of lymphocyte activation was determined at day 7 by identifying the resting and activating lymphocyte regions by FSC vs SSC (left panels). For activation markers see Supplementary Figure 1. The percentage of activated lymphocytes and standard deviation, from 16 independent donors, is plotted in the right panel. **b. Time course of lymphocyte activation.** PBMC were analyzed after five to nine days in co-culture with BCG. **c. Gating strategy for lymphocyte phenotyping.** Once the dead cells were eliminated, NK cells were selected within the whole lymphocyte population in a CD3 vs CD56 plot. Activated CD56^{high} NK cells were gated separately from the rest of CD3⁻CD56⁺ NK cells. The CD3⁺ region was further analyzed for the expression of the $\gamma\delta$ TCR and within each subset, CD4, CD8, and CD56. In some experiments, CD4 and CD8 expression was directly tested in the CD3⁺ region. **d. Lymphocyte proliferation.** PBMC were stained with CellTrace™ Violet before the incubation with BCG, and proliferation was analyzed evaluating the amount of dye per cell by flow cytometry in the different populations. **e. Expression of $\gamma\delta$ T-cells in PBMC from a representative donor.** The $\gamma\delta$ T-cell population is shown within CD3⁺ cells. **f. Expansion of CD3⁺ $\gamma\delta$ T-cells in PBMC.** N = 35 experiments with 33 donors. Statistical analysis was done by one-way ANOVA.

overexpressed in iBCG-treated cells (figure 2f) compared with the rest of the dataset, were captured as a consequence of the great expansion of the $\gamma\delta$ T-cell cluster (Supplementary Table 1).

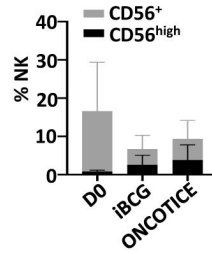
The finding of CD27 expression, together with expression of granzymes already indicated that the expanded population had cytotoxic or pro-inflammatory capacity instead of regulatory, IL17-producing $\gamma\delta$ T-cell characteristics. The LAG3 that appears in many anti-tumor populations could be inhibitory but also released from the cell surface.⁴²

Since our goal was to phenotype the previously described BCG-activated immune cell subpopulations that acquire the capacity to eliminate tumors, in-depth analysis of single cell differential gene expression was done to further characterize the subpopulations containing a productive $\gamma\delta$ TCR chain combination (Figure 3a, b). Six different subclusters were identified and annotated according to differential markers and bibliography (Supplementary Table 1). The great majority of $\gamma\delta$ cells robustly expressed TRDV2 and TRGV9 genes, including subcluster 3 presenting some markers previously

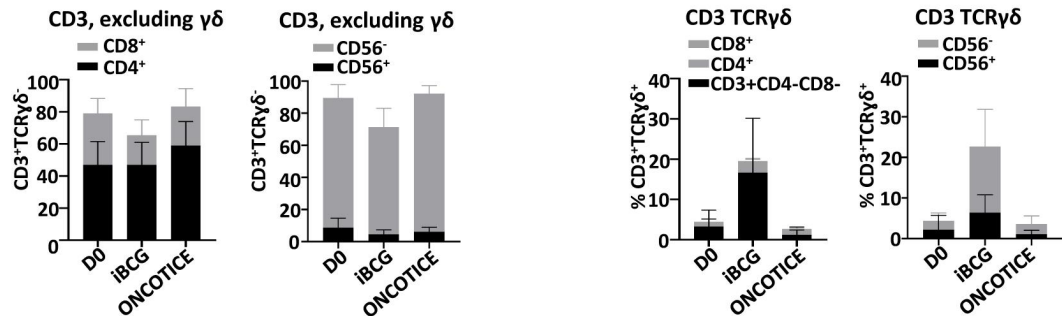
a. Lymphocyte populations, day 7



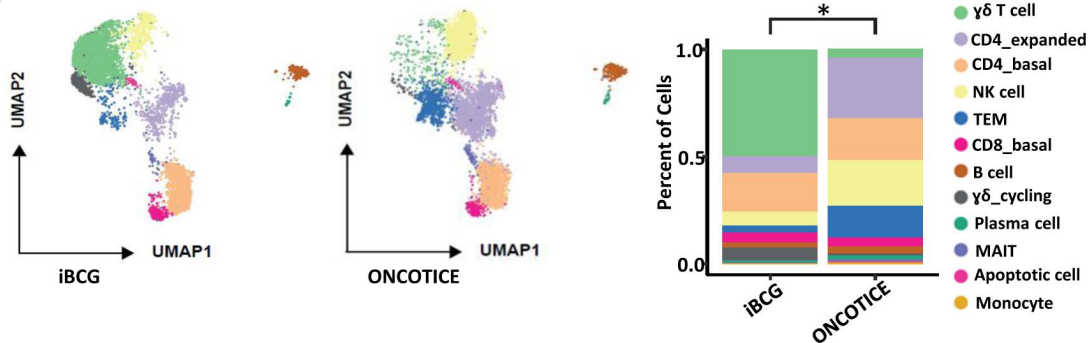
b. NK cells



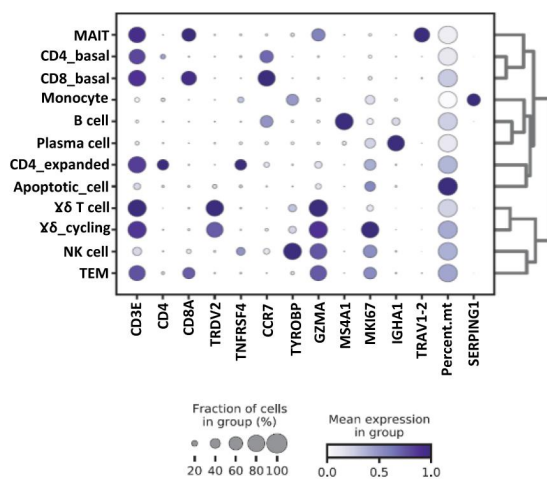
c. T Cell subpopulations



d.



e.



f.

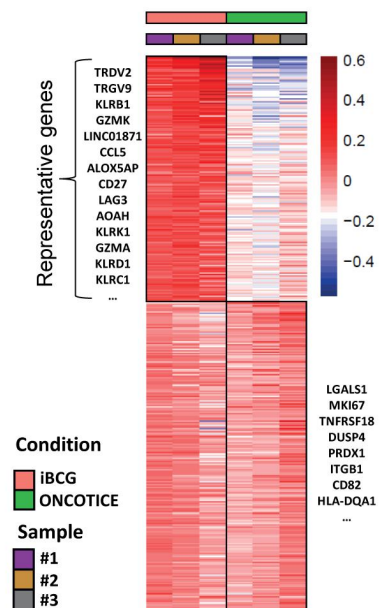


Figure 2. Lymphocyte populations after incubation with BCG. PBMC from healthy donors were incubated with the sub-strains of BCG iBCG or Oncotice at a 6:1 ratio (total bacteria to PBMC). After 7 days in culture, cells in suspension were recovered and analyzed. **a-c. Flow cytometry.** The percentage and standard deviation of the different lymphocyte subpopulations, analyzed by flow cytometry, before and after BCG incubation are plotted. Total lymphocytes (a), NK cells with high or dim CD56 expression (b) and T-cell subpopulations, including γδ T-cells (c) are plotted. This figure includes data from 16 independent donors. **d-f Transcriptomic.** For scRNA-seq

annotated for the TRDV1 population,⁴³ such as FGF2P2 or detectable expression of FCGR3A. However, in this case, this population may reflect a TRDV2 memory-like identity given the expression of KLF2 or SELL. Pseudotime analysis further supported the subcluster annotation, as the trajectory plot separated two main branches enriched in differentiated/resting (subclusters 1, 2, 3) and activated/effector (subclusters 4, 6) $\gamma\delta$ T-cells, respectively (Figure 3c, d). Subcluster 5, and the remaining cells with proliferative capacity, helped to define the start of the trajectory. As mentioned above, and as already described in mice and human systems, most $\gamma\delta$ T-cells expanded in the presence of iBCG expressed NK receptors, such as NCR3 (NKp30), KLRK1 (NKG2D) and several members of the lectin-like receptors (KLR family) (Figure 3e). Comparison of the effector and the well-defined classical TRDV2 subclusters in a volcano plot showed that the effector $\gamma\delta$ T-cell subpopulation differentially increased the expression of TNF, IFNG, GZMB and chemokines (CCL4L2, CCL4, CCL3L1, CCL3), but also the early activation marker CD69 (Figure 3f). Thus, this subcluster was consistent with early/intermediate activation, since the late activation marker CD25 (IL2RA), together with HLA-DR and -DQ molecules, were mainly detected in subcluster 4. Further, cytotoxicity NK receptors were enriched in the effector $\gamma\delta$ T-cell subcluster, in particular FCGR3A (CD16) and NCR3 (NKp30). Interestingly, the orphan receptor KLRC4 (NKG2F) was expressed in most iBCG stimulated $\gamma\delta$ T-cells.

Next, the possible functional capacities of $\gamma\delta$ T-cells generated in the context of iBCG stimulation were explored. Analysis of transcription factors revealed an IFN γ signature in $\gamma\delta$ T-cells with the absence of IL17-related transcription factors (Figure 3g), as characterized by STAT5b, TBX21 expression vs. low STAT3, SOX13.^{44,45} Further, $\gamma\delta$ T-cells could contribute to cytotoxic activity as they expressed molecules such as GZMA (granzyme A) and PRF1 (perforin1) together with increased TNFSF10 (TRAIL), LTA (Lymphotoxin α), and FASLG (Fas-ligand) in the activated and effector $\gamma\delta$ T-cell subclusters (Figure 3h, Supplementary Table 2). Moreover, when cytotoxic signatures were compared at single cell level between the different clusters, $\gamma\delta$ T-cells, and NK cells typically shared similar enrichment scores (Figure 3i).

Expression of NK receptors and cytotoxic molecules on $\gamma\delta$ T-cells was confirmed by flow cytometry analyses (Figure 4). As shown before, the percentage of $\gamma\delta$ T-cells was greatly increased in iBCG treated cultures and around 30% of this population expressed CD56 (Figure 2). Within the CD56⁺ $\gamma\delta$ T-cells, around 70% had the low-affinity Fc γ receptor CD16⁺ (Fc γ RIIIA) on their surface. In contrast, CD56-negative $\gamma\delta$ T-cells mainly lacked CD16 expression (Figure 4a). Confirming the transcriptional analyses showing gene

expression of NKG2D and NCR3 (NKp30), the proteins were also present at the surface of most $\gamma\delta$ T-cells. Interestingly, the fluorescence intensity of NKG2D increased greatly in the co-culture with iBCG, although in some donors only a subpopulation expressed this receptor. CD94/NKG2A proteins were also abundant on the cell surface of the majority of $\gamma\delta$ T-cells, as were CD27 and the cytolytic granule markers granzyme A and perforin (Figure 4b).

In order to understand the requirements of $\gamma\delta$ T-cells to proliferate in the presence of iBCG, experiments were performed comparing PBMC with purified $\gamma\delta$ T-cells. Isolated $\gamma\delta$ T-cells did not expand after BCG stimulation; however, residual $\gamma\delta$ T-cells remaining in PBMC after depletion could still proliferate in response to BCG (Figure 4c). When supernatants from BCG-activated cultures were added to autologous unstimulated PBMC, $\gamma\delta$ T-cells from only one donor expanded (Figure 4d). These data suggest that contact with other populations of leukocytes is required for potent iBCG stimulation of $\gamma\delta$ T-cells.

Taken together, all these data reveal that after iBCG-activation of PBMC, a $\gamma\delta$ T-cell subpopulation expands, mainly V γ 9/V δ 2, expressing CD27 and NK receptors, with cytotoxic and IFN γ -producing capacities, and no evidence of regulatory $\gamma\delta$ T-cell components. These activated effector $\gamma\delta$ T-cells could contribute to tumor elimination, and so their functional capacities were evaluated next.

BCG activation leads to differential patterns of cytokine secretion

The capacity of $\gamma\delta$ T-cells to eliminate tumors was directly evaluated, firstly, identifying the cytokines released *in vitro*; second, by checking their ability to form conjugates; and finally, in tumor cell recognition assays.

Since $\gamma\delta$ T-cells have been shown to have either cytotoxic activity or pro-tumorigenic potential depending on the differential expression of either IFN γ or IL17A,^{30,44,46,47} the secretion of a panel of cytokines, including IFN γ and IL17A, but also IP10, IL6, IL8, IL10, IL12, IL2, IL4, IL17F, IL22, TNF α , IL13, was analyzed by Luminex in several experiments of co-culture of PBMC with BCG (Figure 5a) (Supplementary Figure 8). IFN γ , together with IL6 and TNF α were the soluble factors found at higher concentrations in the supernatants analyzed, while IL4 and IL22 were almost absent. IL8 was present even in untreated cultures. The relative secretion of IFN γ , IL6, TNF α , and IL17A vs IL17F were also tested in comparison with activation of the different lymphocyte populations in the cultures. Principal component analysis (PCA) revealed a higher weight for IL17A in Oncotic treated PBMC, while IFN γ had a stronger weight for iBCG treated PBMC

analysis, three donors were used. Individual data are shown in Supplementary Figure 4D. After quality control (see Materials and Methods, Supplementary Figure 4), raw data from 6383 iBCG-treated PBMC (51% of the pool) and 6097 of Oncotic-treated PBMC (49% of the pool) were combined. Twelve single clusters of lymphocyte subpopulations were identified. **d. Lymphocyte clusters.** UMAP plots represent the 12 clusters identified across the PBMC from 3 donors, stimulated either with iBCG or Oncotic, as indicated (left). The same clusters are expressed as percentage in bar graphs (right), showing the average of the three donors. Individual values are shown in Supplementary Figure 4D. Differences in the proportion of $\gamma\delta$ T-cell cluster between iBCG and Oncotic were significant (paired sample t-test, *p < .05). **e. Cluster annotation.** The graph represents the mean standardized expression values per variable (blue color intensity, as indicated) and the fraction of cells (diameter of the circle) expressing the transcript of the indicated genes (x-axis) within each cluster (y-axis). The cluster labels were added manually. **f. Heat-map.** Heat-map represents the scaled mean expression values of differentially expressed genes across the samples per treatment, showing each donor (sample #1, 2, 3) and treatment (iBCG and oncotic) in different colors.

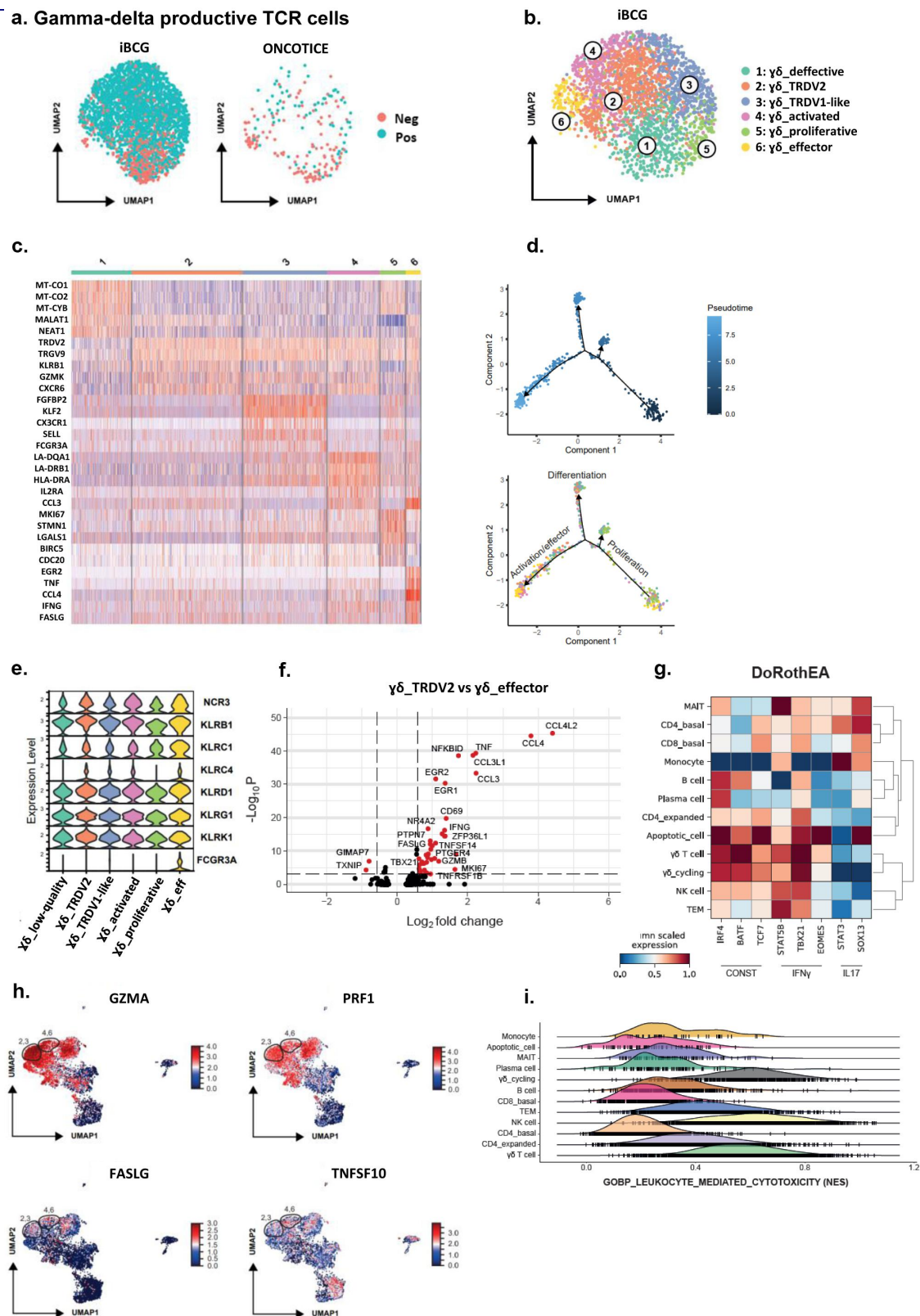
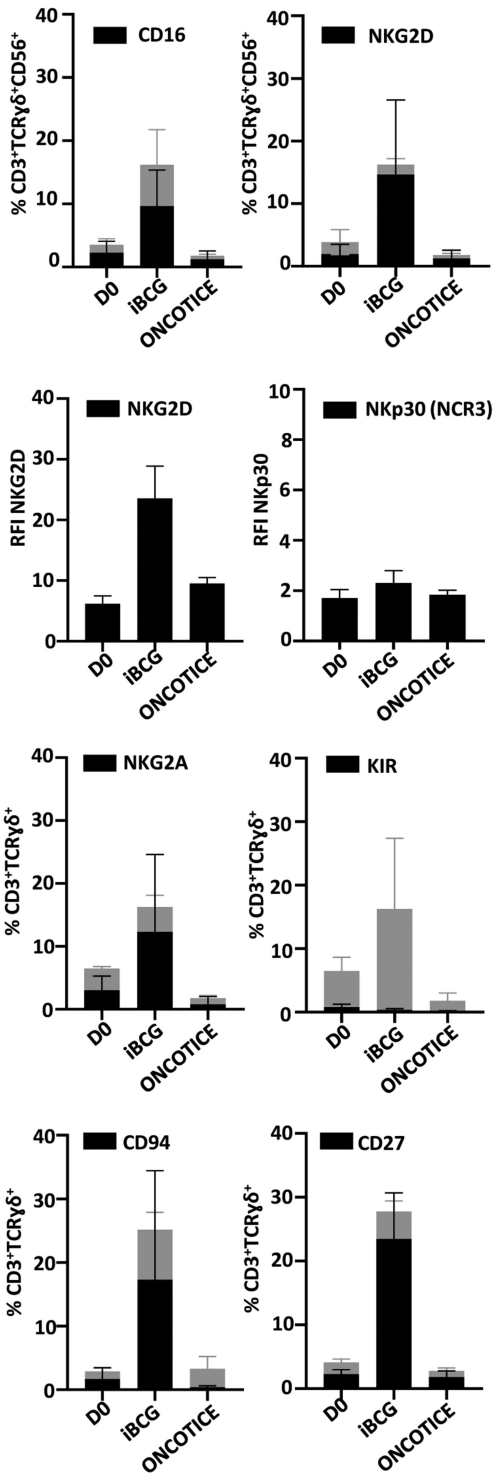
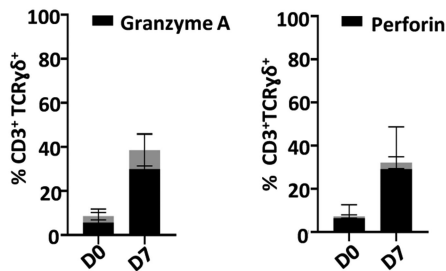


Figure 3. scRNA-seq analysis of $\gamma\delta$ T-cells with a productive TCR chain and their putative functional capacities. **a. $\gamma\delta$ T-cell clusters.** After cluster analysis from Figure 2, $\gamma\delta$ T-cells expressing a productive rearranged TCR chain were further analyzed. UMAP plots represent $\gamma\delta$ T-cells with negative (neg) vs positive (pos) expression of TRDV2/TRGV9 (TCR rearranged chains $\gamma\delta$ 2), in cultures treated with either iBCG or Oncotice, as indicated. **b. Cluster annotation.** UMAP represents the six subclusters identified within iBCG-treated cultures. Subcluster annotation was performed using FindClusters and FindMarkers as described in Methods. The subcluster labels were added manually. **c. Heat-map.** Heat-map represents the scaled expression of differentially expressed genes across the $\gamma\delta$ T-cell subclusters defined in a and b. **d. Trajectory analysis for $\gamma\delta$ T-cell subclusters.** One hundred cells were used per subcluster to perform a trajectory analysis (Monocle2). Cells were represented in a two-dimensional independent space and were colored by pseudotime or by subcluster identity. **e. NK receptors expressed by $\gamma\delta$ T-cell subclusters.** Stacked violin plots represent the mean scaled expression of markers per subcluster. **f. Differential expression of genes between the $\gamma\delta$ _TRDV2 and $\gamma\delta$ _effector subclusters.** Volcano plot represents the genes differentially expressed between the $\gamma\delta$ _TRDV2 and the $\gamma\delta$ _effector subclusters, highlighting in red genes with a $\text{Log}_2\text{FC} > 0.58$ and a Bonferroni adjusted p-value $< 10^{-4}$. **g. Transcription factor inference.** Matrix plot shows the mean standardized transcription factor activity (x-axis) inferred per original cluster (y-axis). **h. Expression of molecules involved in cytotoxicity.** UMAP represents the expression of granzyme A (GZMA), perforin 1 (PRF1), Fas-ligand (FASLG), and TRAIL (TNFSF10) within the entire dataset. Relative localization of $\gamma\delta$ T-cell subclusters 2, 3, 4 and 6 is highlighted. **i. Comparison of the cytotoxic capacity.** Ridge plot represents the normalized enrichment scores (NES) per cluster for the “GOBP_leukocyte_mediated_cytotoxicity” signature.

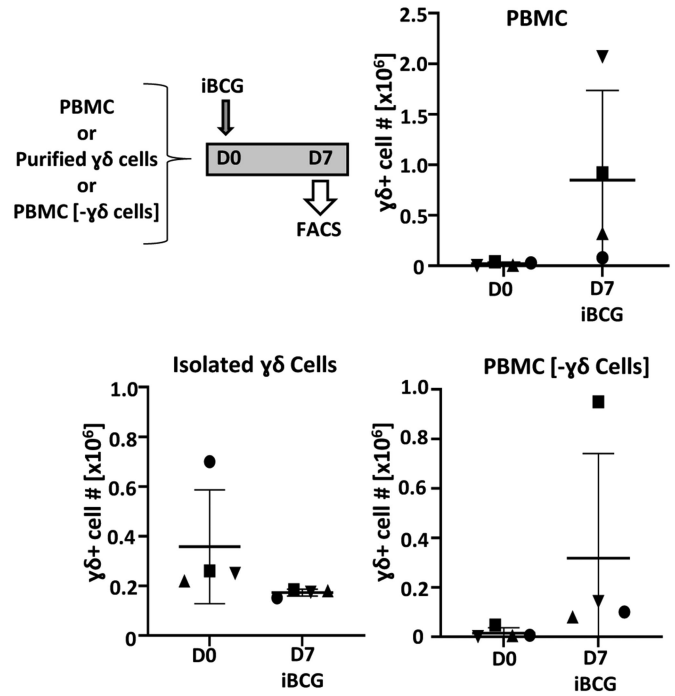
a. NK Receptors in CD3⁺TCRγδ⁺



b. Granzyme A and perforin in CD3⁺TCRγδ⁺



c. Purified γδ T cells + iBCG



d. γδ T cells grown with supernatant from iBCG-stimulated cultures

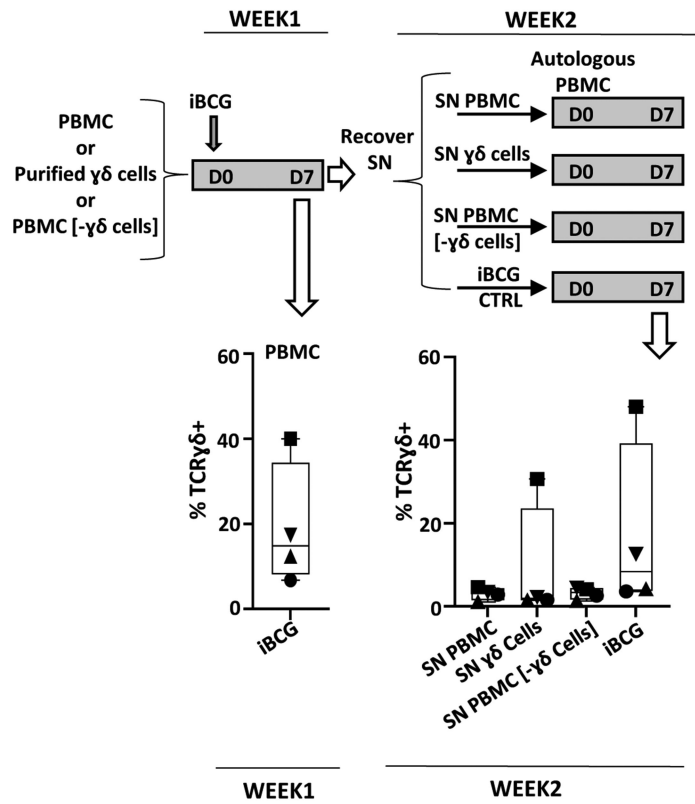


(Figure 5b). However, IL17F was much more abundant (average >500 pg/ml) in BCG-activated cultures than IL17A (average <25 pg/ml). Interestingly, a correlation could be found between IL17A production and proliferation of CD4 T-cells in these cultures (Figure 5c), while increased IFN γ correlated with $\gamma\delta$ T-cell expansion.

Thus, these data confirm that BCG exposure leads to the release of cytokines related to a pro-inflammatory anti-tumor phenotype.

IFN γ -producing $\gamma\delta$ T lymphocytes form conjugates with tumor cells and contribute to their killing

Most BCG-activated NK and $\gamma\delta$ T-cells contained perforin and granzymes as shown in scRNA-seq analysis and confirmed by flow cytometry (Figures 3, 4). Thus, the interaction of these effectors with tumor target cells was evaluated in conjugate formation and degranulation assays. PBMC from healthy donors stimulated with either iBCG or Oncotice for 7 days were used as effector cells against different bladder cancer cell lines (J82, T24, RT-112). The capacity of the effector cells to form conjugates with tumor cells was measured by flow cytometry (Figure 6a, b, c). Both NK and $\gamma\delta$ T-cells were able to form conjugates with bladder cancer cells, while CD3⁺ T-lymphocytes did not. The capacity of lymphocytes to release cytotoxic granules was measured by the expression of surface LAMP1 (CD107a) (Figure 6d, e). Except in certain donors, $\gamma\delta$ T-cells displayed only low degranulation capacity, which was not significantly different from that of non-activated cells. Since tumor killing could use different mechanisms and $\gamma\delta$ T-cells expressed FasL, lymphotoxin and TRAIL, specific cytotoxicity experiments were performed looking at the release of calcein from target cells (specific lysis = target release – spontaneous/max release – spontaneous) (Figure 6f). In these experiments, where the ratio of NK cells to targets was kept constant, the killing of bladder cancer target-cells increased significantly when using BCG-activated cultures compared to unstimulated PBMC. Because two types of effector cells are combined, it is not possible to evaluate the contribution of $\gamma\delta$ T-cells. Since in individual donors with similar percentages of NK cells, a higher fraction of $\gamma\delta$ T-cells does not seem linked to a higher cytotoxicity, we can anticipate that, in this system, most probably NK cells have the predominant anti-tumor cytotoxic activity. In order to investigate the role

of $\gamma\delta$ T-cells in direct cytotoxicity, the culture of these cells after isolation should be investigated.

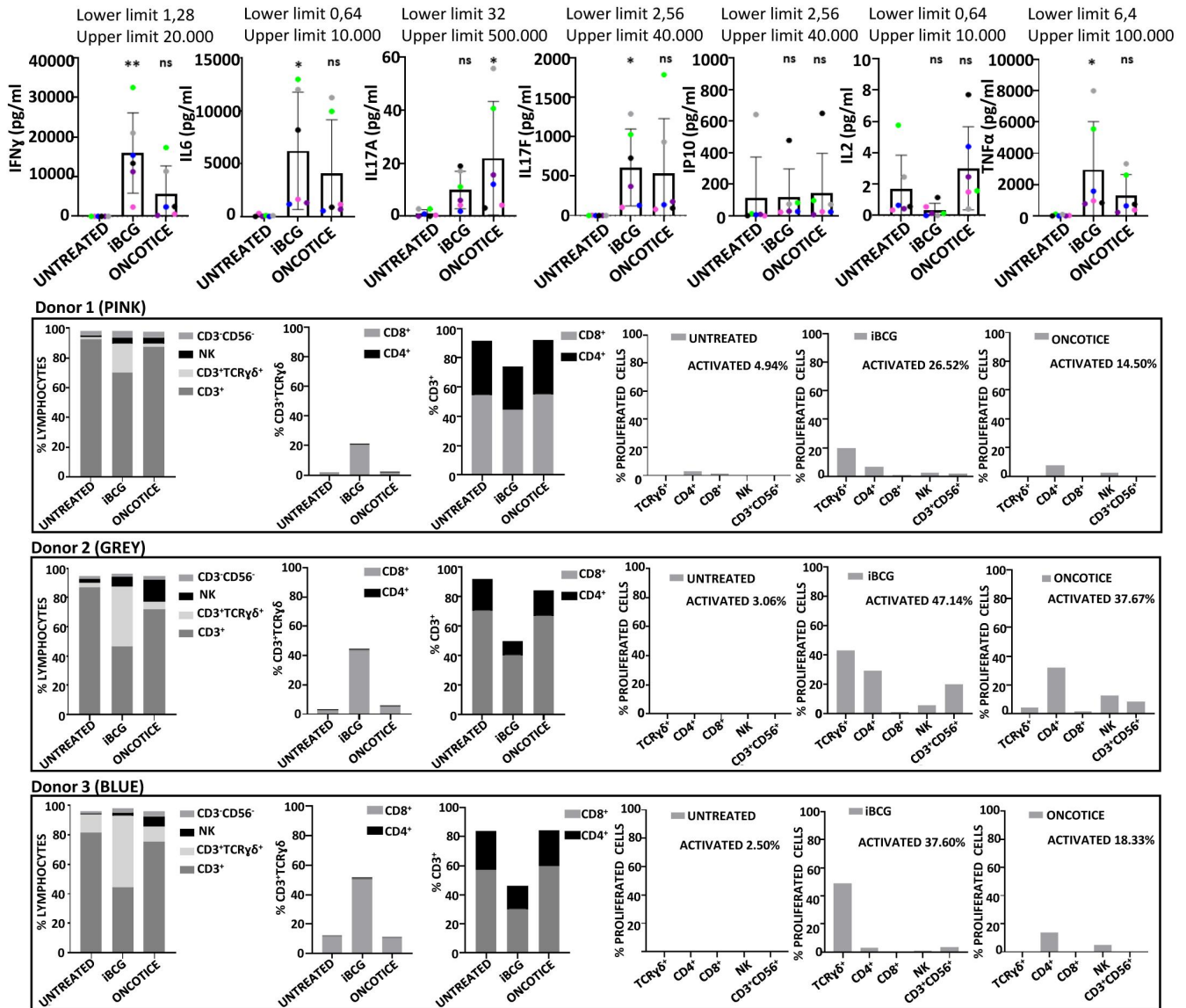
BCG-activated effector cells can be expanded in culture and recognize tumor cells

In order to study the role of $\gamma\delta$ T-cells in more detail, we optimized a method for cytokine-driven expansion of BCG-stimulated lymphocytes. Then, we performed experiments to evaluate the functional capacity of these subpopulations *in vitro*. Combinations of IL12, IL15, IL18, and IL21 have proven to stimulate NK and $\gamma\delta$ T-cell proliferation and cytotoxic activity.²⁴ Moreover, IL15 has been shown to upregulate the expression of CD56 on $\gamma\delta$ T-cells with potent cytotoxic activity. Since our objective was to expand effector cells without causing cell exhaustion, minimal concentrations of cytokines, known to expand NK cells *in vitro* while maintaining function,⁴⁸ were used. In these experiments, PBMC were cultured for a week with BCG, followed by a further incubation with low-doses of IL12, IL15, and IL21. As IL18 is known to promote cytotoxic activity, a low concentration of this cytokine was added to the culture 24 h prior to assay the cytotoxicity (Figure 7a). During the first week in culture, the different lymphocyte populations expanded as previously shown. Addition of cytokines, followed by a further week in culture, doubled cell numbers and, remarkably, the majority of cells expanding in these cultures were innate effector lymphocytes that maintained the phenotype acquired by BCG-activation (Figure 7b). PBMC from five, out of eight donors, resulted in an increase of $\gamma\delta$ T-cells above 100-fold. Cells expanded under these conditions were used as effector in degranulation and cytotoxicity assays, confirming that they kept their capacity to eliminate bladder cells (Figure 7c, d).

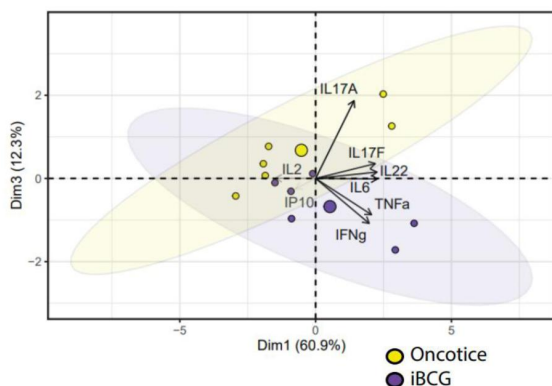
The role of BCG-stimulated cytokine-expanded $\gamma\delta$ T-cells was evaluated next. PBMC from three healthy donors were co-incubated with iBCG for 7 days and, then, $\gamma\delta$ T-cells were purified from the culture and further grown with low doses of cytokines. Surprisingly, $\gamma\delta$ T-cell purification, which yielded 95% purity in unstimulated PMBC, was not so efficient after BCG-activation and some NK cells also appeared in the selected population. For this reason, the percentages of $\gamma\delta$ T-cells at the beginning and after the cytokine culture are shown for each donor. Overall, the number of $\gamma\delta$ T-cells increased, and moderate degranulation was observed in response to co-culture with bladder cancer cells.

Figure 4. Flow cytometry expression of NK receptors and cytotoxic molecules in BCG-activated $\gamma\delta$ T-cells. PBMC from healthy donors were incubated with the substrains of BCG iBCG or Oncotice at a 6:1 ratio (total bacteria to PBMC). After 7 days in culture, cells in suspension were recovered and analyzed by flow cytometry. The percentage of cells expressing each marker and standard deviation are plotted in black. Gray bars represent the average percentage of the CD3⁺TCR $\gamma\delta$ ⁺ subset in the lymphocyte gate. **a. NK Receptors in $\gamma\delta$ T-cells.** The graphs represent the percentage of $\gamma\delta$ T-cells, positive for the indicated marker (black), within the $\gamma\delta$ TCR gate of total lymphocytes. In certain cases, the relative fluorescence intensity (RFI) is shown to analyze the different levels of expression, since the whole population was positive for these markers. An RFI >1 means above the Ig control (RFI = MFI sample/MFI IgG, where MFI is mean fluorescence intensity). **b. Granzyme A and perforin in $\gamma\delta$ T-cells.** N = 6 healthy donors in each case, except for CD27 (seven donors). **c. Purified $\gamma\delta$ T-cells.** $\gamma\delta$ T-cells were negatively selected from $20 \cdot 10^6$ PBMC. Either purified $\gamma\delta$ T-cells or the remaining PBMC ($\gamma\delta$ T-cell-depleted, PBMC [- $\gamma\delta$ cells]) were co-cultured with iBCG for 7 days and analyzed by flow cytometry. The $\gamma\delta$ T-cell number before (D0) and after iBCG culture (D7) are depicted, together with average and standard deviation. For comparison, the activation obtained for each donor after co-culture of PBMC with iBCG was also analyzed. Data from four healthy donors, each one depicted with a different symbol, are shown (purity after $\gamma\delta$ T-cell selection > 95%). **d. $\gamma\delta$ T-cells grown with supernatant from iBCG-stimulated cultures.** Supernatants from the experiment in C were recovered, centrifuged at 10,000x g to eliminate any remaining bacteria, and used to feed a second culture of autologous PBMC. After 1 week in culture, cells were characterized by flow cytometry. The graphs show the percentage of $\gamma\delta$ T-cells expanded in each condition. For comparison, a second co-culture of PBMC with iBCG was also set for each donor.

a. Cytokine release in differentially BCG-activated donors



b. PCA



c. Correlation with cell population

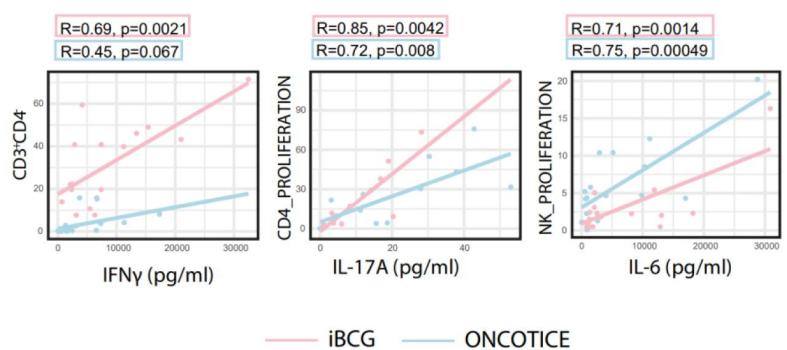


Figure 5. Cytokines released to PBMC cultures after 7-day exposure to BCG. **a. Luminex analysis.** PBMC from six healthy donors were incubated with iBCG or Oncotice as indicated. After 7 days in culture, cell supernatants were recovered for luminex analysis and cells were analyzed by flow cytometry. Cytokine concentrations and standard deviations are depicted in the upper row. Statistical analysis of each treatment with the untreated condition was done by one-way ANOVA. For comparison, flow cytometry data indicating activation and proliferation in the culture from three representative donors (high vs low activation levels) are represented in the three bottom rows: graphs show the percentage of lymphocyte populations obtained at day 7 for each treatment, the percentage of $\gamma\delta$ T-cells, CD3⁺ excluding $\gamma\delta$, and the percentage of populations that proliferated with each treatment (measured by CellTraceTM Violet staining), as indicated. **b. PCA biplot.** Representation of the loadings of principal components. iBCG and Oncotice-treated PBMC were included as separate variables. **c. Correlation of cytokine production and cell population proliferation.** Scatter plot representing the Pearson correlation between parameters (cytokine concentration and cell population that proliferated as measured by CellTraceTM Violet staining). Pink: iBCG; Blue: Oncotice. R and P values were obtained in R using the ggpubr package.

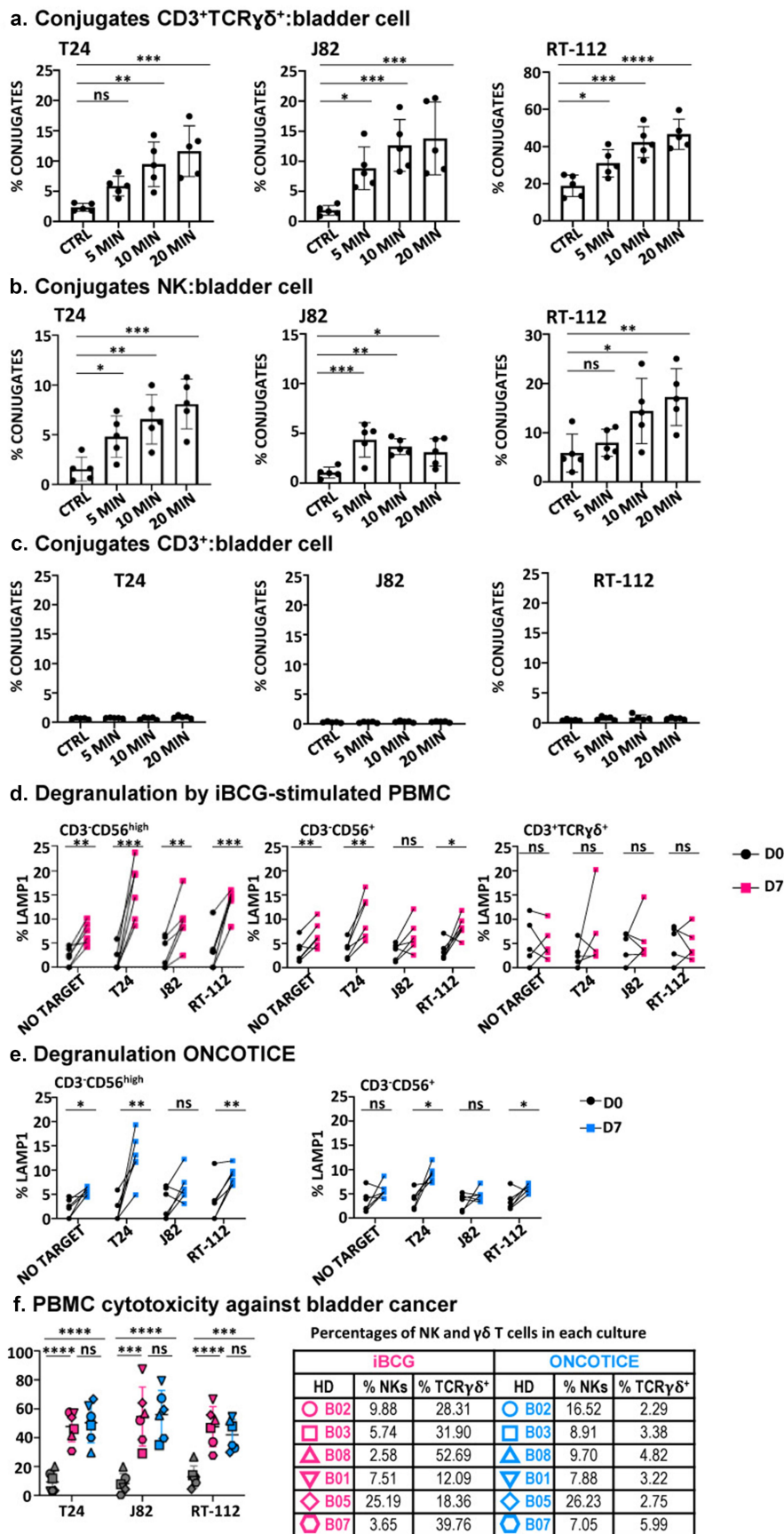


Figure 6. Effector function of PBMC after 7-day exposure to BCG. PBMC from healthy donors were incubated with iBCG or Oncotice as indicated. After 7 days in culture, cells were recovered for their use as effector in functional assays to ensure the recognition and killing of target cells (the bladder cancer cell lines T24, J82, RT-112; K562 cells were used as NK positive control target). **a, b, c. Conjugate formation between effector and target cells.** BCG-treated cells were incubated for 5–20 min with CellTrace™ Violet-dyed target cells at 37°C (except negative control, kept at 4°C). Conjugate formation was measured for double T-cells stained by lymphocyte markers (either CD3⁺TCR $\gamma\delta$ ⁺, CD56⁺ for NK cells or CD3⁺TCR $\gamma\delta$ ⁻ for CD3⁺, presumably TCR $\alpha\beta$) and violet dye. Statistical analysis was performed using one-way ANOVA comparing each condition with the untreated culture (*, $p < .05$; **, $p < .01$; ns, non-significant). **d, e. Degranulation.** The functional capacity of activated NK cells, as

These results demonstrate that induction with BCG, followed by culture in minimal doses of cytokines, allows the expansion of anti-tumor lymphocytes, with NK and $\gamma\delta$ T-cell populations contributing to the specific killing of bladder cancer cell lines. These combinations of effector immune cells could provide the basis for new strategies for generation of adoptive cell therapy. Further improvement of this protocol would be required to obtain high cell numbers of cytotoxic cells in all donors.

Discussion

BCG has been used as a TB vaccine for nearly a hundred years, and as bladder cancer therapy for many decades. Vaccination with BCG has been proposed to stimulate a broad-spectrum immune activation; however, there are still many questions open to fully understand the immune cell populations generated in response to BCG. Importantly, the existence of many BCG sub-strains can affect immunogenicity and add complexity to this topic. Here, to better understand how BCG-activated PBMC contribute to cancer elimination, an in-depth characterization of these lymphocytes has been performed using flow cytometry, scRNA-seq and functional assays. We describe the generation of a $\gamma\delta$ T-cell subpopulation, with anti-tumor cytotoxic and IFN γ -producing capacities, which can be further expanded, together with NK cells, using combinations of cytokines at minimal concentrations. These findings open the door to new approaches for the generation of effector lymphocytes in immunotherapy regimes. Donor heterogeneity and cell numbers will need to be considered together with cytotoxic capacity, for further improvement.

The roles of $\gamma\delta$ T-cells in cancer are a field of very active research. Besides their interest as a diverse innate T-cell population, these cells have a limited TCR polymorphism and, therefore, they could be a source of cells for adoptive cell transfer therapies, even in heterologous settings.^{17,24,49} However, depending on the experimental system, peripheral blood, and tumor infiltrating $\gamma\delta$ T-cells have been reported to have either pro-inflammatory or pro-tumorigenic capacity.^{24,28–31} Thus, definition of the phenotype and function of this cell population is crucial before their use in cellular immunotherapy. Our data show that BCG can expand, in a donor-independent manner in different proportions, NK and $\gamma\delta$ T-cells with functional capacities appropriate for tumor elimination, not just hematological but also solid tumors, such as bladder cancer. In fact, several BCG sub-strains can have this effect. The $\gamma\delta$ T-cells characterized here are reminiscent of the effector memory V γ 9 δ 2 T-cells with a restricted CDR3 oligoclonality, previously described in the context of TB immunity.⁵⁰ The phenotype of these cells was skewed toward CD27 expression and IFN γ production, which

was shown to define the functional capacities of $\gamma\delta$ subsets both in mice and human models of infection.^{37,40}

The characteristics of the PBMC activated by iBCG have been studied in-depth by scRNA-seq and confirmed by flow cytometry. While only minimal differences in the responding NK cells were noted when comparing the two BCG strains used, there was a marked difference in the generation of $\gamma\delta$ T-cells. The existence of differences among BCG sub-strains with regard to interaction with the host is well known, a fact that is clearly evidenced by our results shown in this study. However, further research is required to understand at a molecular level how the small genetic modifications within the different BCGs, as BCG Tice and Moreau, influence the generation of the differential cellular immune responses found here. The receptors expressed by BCG-activated $\gamma\delta$ T-cells, CD27 (TNFRSF7) expression, together with granzymes, TNFSF10 (TRAIL), LTA (Lymphotoxin α), and FASLG (Fas ligand) strongly suggested a cytotoxic function for these cells. This pro-inflammatory effector phenotype was further supported by the IFN γ vs IL17 signature of the transcriptome. As described in the literature for many $\gamma\delta$ T-cell subsets, iBCG-activated $\gamma\delta$ also expressed NK receptors. Thirty percent upregulated CD56 (around 70% of this subset also expressed CD16) and they had on their surface the strong activating NK receptors NKG2D and NCR3, as well as other members of the lectin superfamily receptors. The complete phenotype analyzed by scRNA-seq, together with the cytokine profile confirmed that the $\gamma\delta$ T-cell population proliferating after BCG induction has a CD27⁺ IFN γ proinflammatory non-suppressor phenotype. In fact, IFN γ , together with IL6 and TNF α were found in high concentrations in BCG-activated cultures and the cytotoxic capacity of the cells generated was further evaluated in degranulation, conjugate-formation, and specific cytotoxicity assays. Each one of these experiments confirmed a different functional capacity of the lymphocytes generated by BCG co-culture of PBMC. Altogether, they indicate that BCG stimulates the proliferation of particular subtypes of anti-tumoral innate lymphocytes.

iBCG-activated $\gamma\delta$ T-cells can recognize tumor cells by forming conjugates and increase degranulation against bladder cancer cells. However, while the CD56⁺ subset was able to degranulate, $\gamma\delta$ T-cells contributed to tumor killing in specific cytotoxicity assays against bladder cancer cell lines, presumably via other mechanisms such as TRAIL and FasL.

The nature of ligands stimulating the $\gamma\delta$ T-cells in this system has not been defined, but $\gamma\delta$ T-cells are known to be activated by many different molecules, including intermediates of the cholesterol synthesis pathway, phosphorylated compounds, and bacterial and parasite isoprenoid biosynthesis products.^{3,18,26} Indeed, these compounds are commonly used to expand $\gamma\delta$ T-cells *in vitro*; the use of micromolar amounts of isopentyl pyrophosphate (IPP) and IL2 is used to expand

shown by CD56 upregulation (CD56^{high}) and the rest of the CD3⁺CD56⁺ NK cells (CD56⁺) was analyzed separately, as indicated, as well as degranulation activity of $\gamma\delta$ T-cells (in Oncotice-treated cells this population was scarce, so its analysis is not shown). 25,000 effector cells (normalizing for NK cells) were incubated with 50000 target cells (1:2 E:T ratio) and surface LAMP-1 (CD107a) was measured. Statistical analysis was done by one-way ANOVA. **f. Specific cytotoxicity.** Effector cells were included in cytotoxicity assays against target cells labeled with calcein-AM. Each symbol represents a different healthy donor (HD). Percentages of NK and $\gamma\delta$ T-cells in each culture are included in a table (right). Pink: iBCG; Blue: Oncotice. Statistical analysis was done by one-way ANOVA.

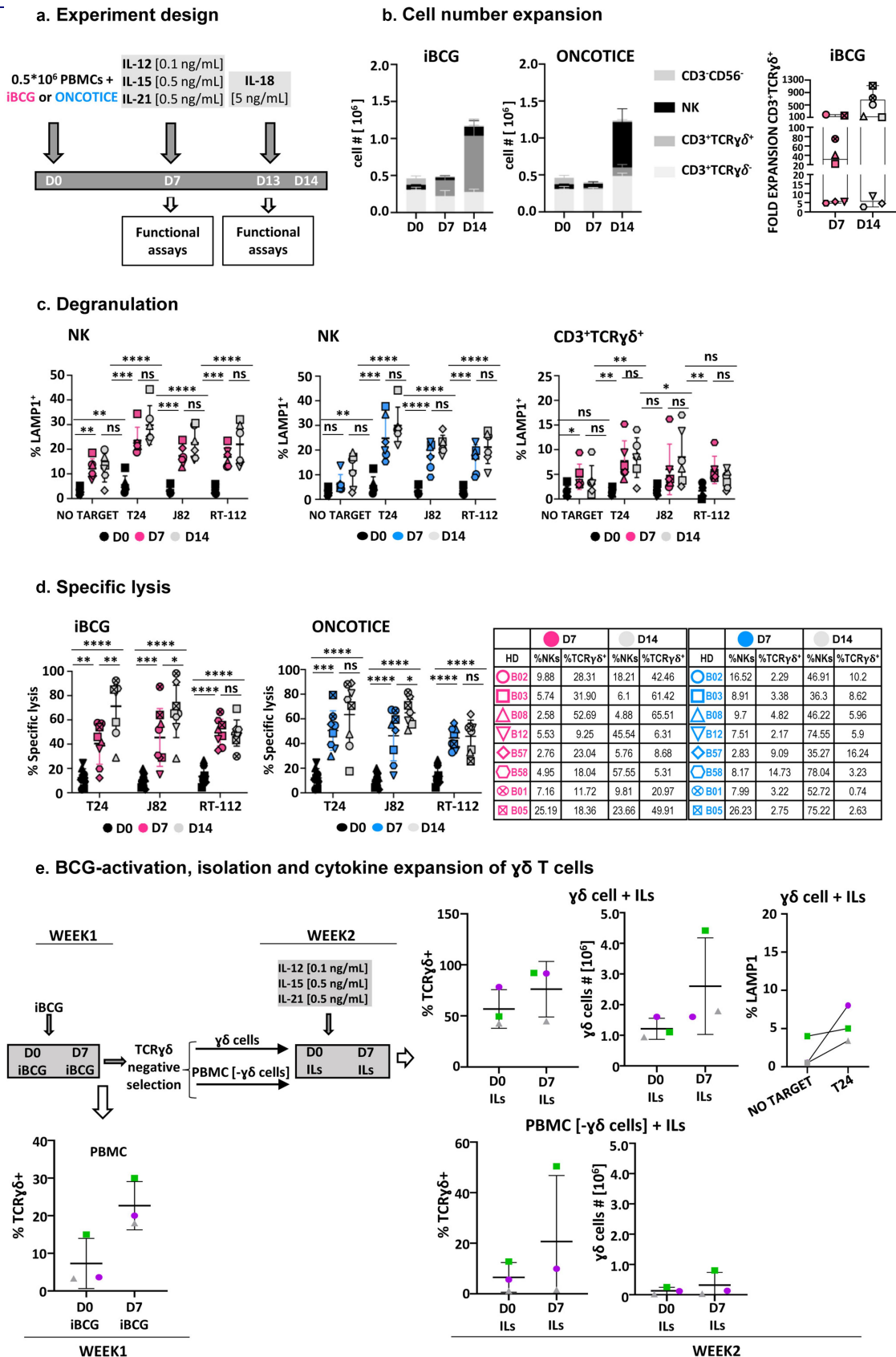


Figure 7. In vitro expansion and isolation of innate effector cells by BCG exposure followed by cytokine treatment. a. Cytokine culture experiment design. PBMC from eight healthy donors were incubated with iBCG (pink) or Oncotice (blue). After 7 days in culture, cells were stimulated with a combination of minimal doses of IL12 (0.1 ng/ml), IL15 (0.5 ng/ml), IL21 (0.5 ng/ml) (gray). One day before analyses, low-dose IL18 (5 ng/ml) was added. **b. Cell numbers.** At the end of the incubation time, cells were counted and the percentage of each population within the live cell gate was analyzed by flow cytometry (left panel). The fold-expansion of CD3⁺ γδ T-cells after 7 and 14 days is shown (right panel). Each symbol represents a different healthy donor (HD). **c. Degranulation.** PBMC from 6 healthy donors were used as effector against target cells (the bladder cancer cell lines T24, J82, RT-112; K562 cells were used as NK positive control target), as indicated. The functional capacity of NK cells and γδ T-cells were analyzed separately (in Oncotice-treated cells the latter population was scarce, so its analysis is not shown). 12500 effector cells (normalizing for NK cells) were incubated with 25000 target cells (1:2 E:T ratio) and surface LAMP-1 (CD107a) was measured. Pink: iBCG; Blue: Oncotice; Grey: minimal dose cytokines,

V γ 9V δ 2 $\gamma\delta$ T-cells from peripheral blood. This phosphoantigen can be generated after monocyte incorporation of amino-bisphosphonates, such as zoledronic acid (ZOL), also used to activate V γ 9V δ 2 T-cells *in vitro*.⁵¹ It is now clear that different concentrations of phosphoantigens, when combined with particular cytokines, can give rise to completely different repertoires of $\gamma\delta$ T-cells, in a process that also depends on cross-talk with other peripheral blood cell populations.^{24,52} For example, earlier data obtained using nonpathogenic *Salmonella* engineered to stimulate $\gamma\delta$ T-cell production via overexpression of PP metabolites generated V γ 2 δ 2 cells.⁵³ ZOL together with IL2 has been used for expansion of CD27⁻ $\gamma\delta$ T-cells expressing IFN γ , TNF α , perforin, granzyme B, FASL, and TRAIL that only proliferated for 14 days.⁵⁴ Butyrophilin binding to phosphoantigens generated by other cell types could also be involved in $\gamma\delta$ T-cell expansion.^{52,55} However, in the work presented here, we did not test the molecules involved in stimulation of this subset after BCG co-culture. On the other hand, neutrophil uptake of ZOL inhibits $\gamma\delta$ T-cells and, while IPP-activated $\gamma\delta$ T-cells express CD25 and CD69, they do not proliferate further if they are isolated,²⁵ reflecting, again, the complexity of the system.

Although it was not the goal of this work, the generation of anti-tumor $\gamma\delta$ T-cells with BCG could also provide a tool for emerging cellular therapies. Several methods for the expansion of $\gamma\delta$ T-cells for adoptive cell therapy are under investigation since a very high number of cells are required.²⁷ In general, a 10-fold increase in $\gamma\delta$ T-cells was obtained when using ZOL (see Table 1).⁵¹ These different methods include, on many occasions, high doses of cytokines, in general IL2, and in some cases, the protocol involves depletion of $\alpha\beta$ T cells. In the case of BCG-stimulation, no depletion was done and minimal doses of cytokines were used, representing a clear advantage, both in time and expense. It is important to highlight that not all the donors respond with the same intensity to generate $\gamma\delta$ T-cells. Heterogeneity between donors was explored when treating PBMC with ZOL+IL2 in Burnham et al.⁴⁹ In this paper, non-expander donors could generate $\gamma\delta$ T-cells after the addition of IL15 and/or IL21. The average expansion with BCG, followed by minimal doses of cytokines, was around 100-fold, and three out of eight donors had a 500-fold expansion, suggesting that the protocol could be improved by adjusting the identity, timing, or concentration of cytokines. During the preparation of this paper, a report combining BCG and ZOL was published, suggesting also an advantage of the inclusion of BCG in the anti-tumor phenotype of the resulting cells, compared to ZOL that increased the exhaustion markers CD57, PD1, and TIM3.⁵⁶ These markers were not detected in our hands in BCG-treated PBMC. Another consideration refers to the use

of combinations of NK + $\gamma\delta$ T-cells as recently reported⁵⁷ because they seem to synergize for a good anti-tumor response. However, it will be important to consider the effects and doses of the different cytokines in these systems. The use of IL2 can strongly activate, but also exhaust a number of populations.⁵⁸ Moreover, if used in patients, it could cause toxicity. Thus, other cytokine combinations have been explored, and the cytokines IL12, IL15, IL18, and IL21 have been shown to contribute to the cytolytic activity of $\gamma\delta$ T-cells, in different contexts.⁵⁹ We have also shown here that the use of 10–100 times lower concentrations of these cytokines avoids cell exhaustion while expanding $\gamma\delta$ T-cell and NK cell numbers.

In conclusion, the combination of one-week of iBCG activation followed by minimal doses of cytokines doubled the number of PBMC and over 70% of these cells were NK and $\gamma\delta$ T-cell effectors with the same anti-tumor properties as the initial BCG-activated population. Thus, these conditions generate and expand cytotoxic effector cells whose capacity to further proliferate *in vitro* should be explored.

Acknowledgments

The authors would like to thank M. Muñoz (Crick Institute, UK) for a critical review of the manuscript; L. Martínez-Piñeiro (H. La Paz, Madrid) for BCG; A. Dopazo and the Genomics Unit of the National Centre for Cardiovascular Research (CNIC, Madrid, Spain) for their advice on scRNAseq analysis. The group of MVG belongs to the research network “Conexión cancer”-CSIC. MJF and AFGJ are registered PhD students at the Molecular Biosciences doctoral program of the Universidad Autónoma de Madrid (UAM).

Disclosure statement

EP, ER, and IM are employees of Biofabri, S.L.

Funding

This work was supported by the Spanish Ministry of Science and Innovation under Grants (RTC-2017-6379-1, RTI2018-093569-B-I00, PID2021-123795OB-I00 [Ministerio de Ciencia, Innovación y Universidades (MCIU)/Agencia Estatal de Investigación (AEI)/European Regional Development Fund (FEDER, EU)], SAF2017-83265-R (HTR); and the regional government of Madrid [COMUNIDAD DE MADRID S2017/BMD-3733-2 (MVG)]; MJF is a fellow of the INPhINIT Doctoral Programme from La Caixa Foundation (LCF/BQ/DI19/11730039). AFGJ is a recipient of a fellowship (FPU18/01698) from the Spanish Ministry of Science and Education.

ORCID

Mar Valés-Gómez  <http://orcid.org/0000-0001-7424-3206>

target as indicated. Statistical analysis was done by one-way ANOVA. **d. Specific cytotoxicity.** Effector cells were included in cytotoxicity assays against target cells labeled with calcein-AM. 50000 effector cells (normalizing for NK cells) were incubated with 10000 target cells (5:1 E:T ratio). Pink: iBCG; Blue: Oncotic; Grey: minimal-dose cytokines. Statistical analysis was done by one-way ANOVA. **e. BCG-activation, purification and minimal-dose cytokine expansion of $\gamma\delta$ T-cells followed by degranulation experiments.** PBMC from three healthy donors were incubated with iBCG. After 7 days in culture, $\gamma\delta$ T-cells were subjected to selection using the MACS system and 10⁶ cells were stimulated with a combination of low-dose IL12 (0.1 ng/ml), IL15 (0.5 ng/ml), IL21 (0.5 ng/ml) and kept in culture for another week and analyzed, then, by flow cytometry. Data from three healthy donors, each one depicted with a different symbol, are shown. Because purity of the $\gamma\delta$ T-cell selection decreased after BCG-activation, compared to the 95% purity obtained when using fresh cells, the $\gamma\delta$ T-cell number before (D0) and after iBCG culture (D7), as well as those obtained after selection and cytokine activation are depicted separately. The average and standard deviation are shown in each graph. $\gamma\delta$ T-cells (average 75% purity), obtained after BCG-activation and further expansion with low-dose cytokines, were used as effector cells in degranulation assays. The graph represents the percentage of LAMP-1 (CD107a) measured by flow cytometry.

Data availability statement

R code related to the main scRNA-seq figures can be found at https://github.com/algarji/BCG_scRNA-seq.

Raw data of the scRNA-seq analysis will be found at GEO (<https://www.ncbi.nlm.nih.gov/geo/>)

Author contributions

GE, MJF, AFGJ, CRV, HTR acquired, analyzed, and interpreted data
EP, NA, ER, IM provided mycobacterial reagents
NA, CM, ER, IM, and MVG provided material support
GE, MJF, and MVG wrote the manuscript
MVG supervised the study
All authors participated in critical revisions of the article

References

- Calmette A, Bocquet A, Negre L. Contribution à l'étude du bacille tuberculeux bilie. *Ann Inst Pasteur*. 1921;9:561–570.
- Gandhi NM, Morales A, Lamm DL. Bacillus calmette-Guerin immunotherapy for genitourinary cancer. *BJU International*. 2013 Aug;112(3):288–297. doi:10.1111/j.1464-410X.2012.11754.x.
- Foster M, Hill PC, Setiabudiawan TP, Koeken VACM, Alisjahbana B, Crevel R. BCG-induced protection against Mycobacterium tuberculosis infection: evidence, mechanisms, and implications for next-generation vaccines. *Immunol Rev*. 2021 Mar 12;301(1):122–144. doi:10.1111/imr.12965.
- Behr MA, Small PM. A historical and molecular phylogeny of BCG strains. *Vaccine*. 1999 Feb 26;17(7–8):915–922. doi:10.1016/S0264-410X(98)00277-1.
- Gan C, Mostafid H, Khan MS, Lewis DJM. BCG immunotherapy for bladder cancer—the effects of substrain differences. *Nat Rev Urol*. 2013 Oct;10(10):580–588. doi:10.1038/nrurol.2013.194.
- Zhang L, Ru HW, Chen FZ, Jin CY, Sun RF, Fan XY, et al. Variable virulence and efficacy of BCG vaccine strains in mice and correlation with genome polymorphisms. *Mol Ther*. 2016 Feb;24(2):398–405. doi:10.1038/mt.2015.216.
- Zufferey C, Germano S, Dutta B, Ritz N, Curtis N. The contribution of non-conventional T cells and NK cells in the mycobacterial-specific IFN γ response in bacille calmette-guerin (BCG)-immunized infants. *PloS one*. 2013;8(10):e77334. doi:10.1371/journal.pone.0077334.
- Roy A, Eisenhut M, Harris RJ, Gan C, Mostafid H, Khan MS, Lewis DJM. Effect of BCG vaccination against Mycobacterium tuberculosis infection in children: systematic review and meta-analysis. *Bmj*. 2014 Aug 5;349(aug04 5):g4643. doi:10.1136/bmj.g4643.
- Mazurek GH, Jereb J, Vernon A, LoBue P, Goldberg S, Castro K. Updated guidelines for using interferon gamma release assays to detect mycobacterium tuberculosis infection - United States, 2010. *MMWR Recomm Rep*. 2010 Jun 25;59(RR-5):1–25.
- Rozot V, Nemes E, Geldenhuys H, Musvosvi M, Toefy A, Rantangee F, Makhetha L, Erasmus M, Bilek N, Mabwe S, et al. Multidimensional analyses reveal modulation of adaptive and innate immune subsets by tuberculosis vaccines. *Commun Biol*. 2020 Oct 9;3(1):563. doi:10.1038/s42003-020-01288-3.
- Roy Chowdhury R, Vallania F, Yang Q, Lopez Angel CJ, Darboe F, Penn-Nicholson A, Rozot V, Nemes E, Malherbe ST, Ronacher K, et al. A multi-cohort study of the immune factors associated with M. tuberculosis infection outcomes. *Nature*. 2018 Aug;560(7720):644–648. doi:10.1038/s41586-018-0439-x.
- Garcia-Cuesta EM, Esteso G, Ashiru O, López-Cobo S, Álvarez-Maestro M, Linares A, Ho MM, Martínez-Piñero L, T. Reyburn H, Valés-Gómez M, et al. Characterization of a human anti-tumoral NK cell population expanded after BCG treatment of leukocytes. *Oncoimmunology*. 2017;6(4):e1293212. doi:10.1080/2162402X.2017.1293212.
- Suliman S, Geldenhuys H, Johnson JL, Hughes JE, Smit E, Murphy M, Toefy A, Lerumo L, Hopley C, Pienaar B, et al. Bacillus Calmette–Guérin (BCG) revaccination of adults with latent mycobacterium tuberculosis infection induces long-lived BCG-Reactive NK cell responses. *J Immunol*. 2016 Aug 15;197(4):1100–1110. doi:10.4049/jimmunol.1501996.
- O'Neill LAJ, Netea MG. BCG-induced trained immunity: can it offer protection against COVID-19? *Nat Rev Immunol*. 2020 Jun;20(6):335–337. doi:10.1038/s41577-020-0337-y.
- Mujal AM, Delconte RB, Sun JC. Natural killer cells: from innate to adaptive features. *Annu Rev Immunol*. 2021 Apr 26;39(1):417–447. doi:10.1146/annurev-immunol-101819-074948.
- Della Chiesa M, De Maria A, Muccio L, Bozzano F, Sivori S, Moretta L. Human NK cells and herpesviruses: mechanisms of recognition, response and adaptation. *Front Microbiol*. 2019;10:2297. doi:10.3389/fmicb.2019.02297.
- Van Rhijn I, Moody DB. Donor unrestricted T cells: a shared human T cell response. *J Immunol*. 2015 Sep 1;195(5):1927–1932. doi:10.4049/jimmunol.1500943.
- Kulicke CA, Lewinsohn DA, Lewinsohn DM. Clonal enrichments of Vdelta2- gammadelta T cells in Mycobacterium tuberculosis-infected human lungs. *J Clin Invest*. 2020 Jan 2;130(1):68–70. doi:10.1172/JCI133119.
- Ogongo P, Steyn AJ, Karim F, Dullabh KJ, Awala I, Madansein R, Leslie A, Behar SM. Differential skewing of donor-unrestricted and gammadelta T cell repertoires in tuberculosis-infected human lungs. *J Clin Invest*. 2020 Jan 2;130(1):214–230. doi:10.1172/JCI130711.
- Esteso G, Aguilo N, Julian E, Ashiru O, Ho MM, Martín C, Valés-Gómez M. Natural killer anti-tumor activity can be achieved by in vitro incubation with heat-killed BCG. *Front Immunol*. 2021;12:622995. doi:10.3389/fimmu.2021.622995.
- Wagner JA, Rosario M, Romee R, Berrien-Elliott MM, Schneider SE, Leong JW, Sullivan RP, Jewell BA, Becker-Hapak M, Schappe T, et al. CD56bright NK cells exhibit potent antitumor responses following IL-15 priming. *J Clin Invest*. 2017 Nov 1;127(11):4042–4058. doi:10.1172/JCI90387.
- Smith SG, Kleinnijenhuis J, Netea MG, Dockrell HM. Whole blood profiling of bacillus calmette-guerin-induced trained innate immunity in infants identifies epidermal growth factor, IL-6, platelet-derived growth factor-AB/BB, and natural killer cell activation. *Front Immunol*. 2017;8:644. doi:10.3389/fimmu.2017.00644.
- Kleinnijenhuis J, Quintin J, Preijers F, Joosten LAB, Jacobs C, Xavier RJ, van der Meer JWM, van Crevel R, Netea MG. BCG-induced trained immunity in NK cells: role for non-specific protection to infection. *Clin Immunol*. 2014 Dec;155(2):213–219. doi:10.1016/j.clim.2014.10.005.
- Kabelitz D, Serrano R, Kouakanou L, Peters C, Kalyan S. Cancer immunotherapy with gammadelta T cells: many paths ahead of us. *Cell Mol Immunol*. 2020 Sep;17(9):925–939. doi:10.1038/s41423-020-0504-x.
- Fowler DW, Copier J, Wilson N, Dalgleish AG, Bodman-Smith MD. Mycobacteria activate gammadelta T-cell anti-tumour responses via cytokines from type 1 myeloid dendritic cells: a mechanism of action for cancer immunotherapy. *Cancer Immunol Immunother*. 2012 Apr;61(4):535–547. doi:10.1007/s00262-011-1121-4.
- Wesch D, Marx S, Kabelitz D. Comparative analysis of alpha beta and gamma delta T cell activation by Mycobacterium tuberculosis and isopentenyl pyrophosphate. *Eur J Immunol*. 1997 Apr;27(4):952–956. doi:10.1002/eji.1830270422.
- Saura-Esteller J, de Jong M, King LA, Ensing E, Winograd B, de Grujil TD, et al. Gamma delta T-cell based cancer immunotherapy: past-present-future [Mini Review]. *Frontiers in Immunology*. 2022 June 16;13:13.
- Zhao Y, Niu C, Cui J. Gamma-delta (gammadelta) T cells: friend or foe in cancer development? *J Transl Med*. 2018 Jan 10;16(1):3. doi:10.1186/s12967-017-1378-2.

29. Li Y, Li G, Zhang J, Wu X, Chen X. The dual roles of human gammadelta T cells: anti-Tumor or tumor-promoting. *Front Immunol.* 2020;11:619954. doi:10.3389/fimmu.2020.619954.
30. Chabab G, Barjon C, Bonnefoy N, Lafont V. Pro-tumor gamma-delta T cells in human cancer: polarization, mechanisms of action, and implications for therapy. *Front Immunol.* 2020;11:2186. doi:10.3389/fimmu.2020.02186.
31. Caron J, Ridgley LA, Bodman-Smith M. How to train your dragon: harnessing gamma delta T cells antiviral functions and trained immunity in a pandemic era. *Front Immunol.* 2021;12:666983. doi:10.3389/fimmu.2021.666983.
32. Ritz N, Hanekom WA, Robins-Browne R, Britton WJ, Curtis N. Influence of BCG vaccine strain on the immune response and protection against tuberculosis. *FEMS Microbiol Rev.* 2008 Aug;32(5):821–841. doi:10.1111/j.1574-6976.2008.00118.x.
33. van Dongen JJ, Langerak AW, Bruggemann M, Evans PAS, Hummel M, Lavender FL, Delabesse E, Davi F, Schuurin E, Garcia-Sanz R, et al. Design and standardization of PCR primers and protocols for detection of clonal immunoglobulin and T-cell receptor gene recombinations in suspect lymphoproliferations: report of the BIOMED-2 Concerted Action BMH4-CT98-3936. *Leukemia.* 2003 Dec;17(12):2257–2317. doi:10.1038/sj.leu.2403202.
34. Krangel MS. Mechanics of T cell receptor gene rearrangement. *Curr Opin Immunol.* 2009 Apr;21(2):133–139. doi:10.1016/j.coi.2009.03.009.
35. Boria I, Cotella D, Dianzani I, Santoro C, Sblattero D. Primer sets for cloning the human repertoire of T cell receptor variable regions. *BMC Immunol.* 2008 Aug 29;9(1):50. doi:10.1186/1471-2172-9-50.
36. Spencer CT, Abate G, Sakala IG, Xia M, Truscott SM, Eickhoff CS, Linn R, Blazevic A, Metkar SS, Peng G, et al. Granzyme A produced by gamma(9)delta(2) T cells induces human macrophages to inhibit growth of an intracellular pathogen. *PLoS Pathog.* 2013 Jan;9(1):e1003119. doi:10.1371/journal.ppat.1003119.
37. Qin G, Liu Y, Zheng J, Xiang Z, Ng IHY, Malik Peiris JS, Lau Y-L, Tu W. Phenotypic and functional characterization of human gammadelta T-cell subsets in response to influenza A viruses. *J Infect Dis.* 2012 Jun;205(11):1646–1653. doi:10.1093/infdis/jis253.
38. Liu Y, Zhang C. The role of human gammadelta T cells in anti-tumor immunity and their potential for cancer immunotherapy. *Cells.* 2020 May 13;9(5):1206. doi:10.3390/cells9051206.
39. Becht E, McInnes L, Healy J, Dutertre C-A, Kwok IWH, Ng LG, Ginhoux F, Newell EW. Dimensionality reduction for visualizing single-cell data using UMAP. *Nature Biotechnology.* 2018 Dec 3; doi:10.1038/nbt.4314.
40. Ribot JC, deBarros A, Pang DJ, Neves JF, Peperzak V, Roberts SJ, Girardi M, Borst J, Hayday AC, Pennington DJ, et al. CD27 is a thymic determinant of the balance between interferon-gamma- and interleukin 17-producing gammadelta T cell subsets. *Nat Immunol.* 2009 Apr;10(4):427–436. doi:10.1038/ni.1717.
41. Hendriks J, Gravestein LA, Tesselaar K, van Lier RA, Schumacher TN, Borst J. TN, Borst J. CD27 is required for generation and long-term maintenance of T cell immunity. *Nat Immunol.* 2000 Nov;1(5):433–440. doi:10.1038/80877.
42. Maruhashi T, Sugiura D, Okazaki IM, Okazaki T. LAG-3: from molecular functions to clinical applications. *J Immunother Cancer.* 2020 Sep;8(2):e001014. doi:10.1136/jitc-2020-001014.
43. Pizzolato G, Kaminski H, Tosolini M, Franchini DM, Pont F, Martins F, et al. Single-cell RNA sequencing unveils the shared and the distinct cytotoxic hallmarks of human TCRVdelta1 and TCRVdelta2 gammadelta T lymphocytes. *Proc Natl Acad Sci U S A.* 2019 Jun 11;116(24):11906–11915. doi:10.1073/pnas.1818488116.
44. Park JH, Lee HK. Function of gammadelta T cells in tumor immunology and their application to cancer therapy. *Exp Mol Med.* 2021 Mar;53(3):318–327. doi:10.1038/s12276-021-00576-0.
45. Parker ME, Ciofani M. Regulation of gammadelta T cell effector diversification in the thymus. *Front Immunol.* 2020;11:42. doi:10.3389/fimmu.2020.00042.
46. Patil RS, Shah SU, Shrikhande SV, Goel M, Dikshit RP, Chiplunkar SV. IL17 producing gammadelta T cells induce angiogenesis and are associated with poor survival in gallbladder cancer patients. *Int J Cancer.* 2016 Aug 15;139(4):869–881. doi:10.1002/ijc.30134.
47. Lawand M, Dechanet-Merville J, Dieu-Nosjean MC. Key features of GAMMA-Delta T-Cell subsets in human diseases and their immunotherapeutic Implications. *Front Immunol.* 2017;8:761. doi:10.3389/fimmu.2017.00761.
48. Felgueres MJ, Esteso G, Vales-Gomez M. Low dose cytokine-activated characterization and proliferation of anti-tumoral NK cells. Abstract at the Society for Natural Immunity Meeting NK2022: 50 Years of NK Cells, Bonita Springs, FL. 2022.
49. Burnham RE, Zoine JT, Story JY, Garimalla SN, Gibson G, Rae A, et al. Characterization of donor variability for gammadelta T cell ex vivo expansion and development of an allogeneic gammadelta T cell immunotherapy. *Front Med (Lausanne).* 2020;7:588453. doi:10.3389/fmed.2020.588453.
50. Spencer CT, Abate G, Blazevic A, Hoft DF. Only a subset of phosphoantigen-Responsive γ δ 2 T cells mediate protective tuberculosis immunity. *J Immunol.* 2008 Oct 1;181(7):4471–4484. doi:10.4049/jimmunol.181.7.4471.
51. Wang RN, Wen Q, He WT, Yang JH, Zhou CY, Xiong WJ, et al. Optimized protocols for gammadelta T cell expansion and lentiviral transduction. *Mol Med Rep.* 2019 Mar;19(3):1471–1480. doi:10.3892/mmr.2019.9831.
52. Nerdal PT, Peters C, Oberg HH, Zlatev H, Lettau M, Quabius ES, Sousa S, Gonnermann D, Auriola S, Olive D, et al. Butyrophilin 3A/CD277-dependent activation of human gammadelta T cells: accessory cell capacity of distinct leukocyte populations. *J Immunol.* 2016 Oct 15;197(8):3059–3068. doi:10.4049/jimmu.1600913.
53. Workalemahu G, Wang H, Puan KJ, Nada MH MH, Kuzuyama T, Jones BD, et al. Metabolic engineering of Salmonella vaccine bacteria to boost human Vgamma2Vdelta2 T cell immunity. *J Immunol.* 2014 Jul 15;193(2):708–721. doi:10.4049/jimmunol.1302746.
54. Kondo M, Sakuta K, Noguchi A, Ariyoshi N, Sato K, Sato S, Sato K, Hosoi A, Nakajima J, Yoshida Y, et al. Zoledronate facilitates large-scale ex vivo expansion of functional gammadelta T cells from cancer patients for use in adoptive immunotherapy. *Cytotherapy.* 2008;10(8):842–856. doi:10.1080/14653240802419328.
55. Rigau M, Ostrouska S, Fulford TS, Johnson DN, Woods K, Ruan Z, McWilliam HEG, Hudson C, Tutuka C, Wheatley AK, et al. Butyrophilin 2A1 is essential for phosphoantigen reactivity by gammadelta T cells. *Science.* 2020 Feb 7;367(6478). doi:10.1126/science.aay5516.
56. Fenn J, Ridgley LA, White A, Sarfas C, Dennis M, Dalglish A, Reljic R, Sharpe S, Bodman-Smith M. Bacillus Calmette-Guerin (BCG) induces superior anti-tumour responses by Vdelta2+ T cells compared with the aminobisphosphonate drug zoledronic acid. *Clin Exp Immunol.* 2022 Jun 23;208(3):301–315. doi:10.1093/cei/uxac032.
57. Jonus HC, Burnham RE, Ho A, Pilgrim AA, Shim JJ, Doering CB, et al. Dissecting the cellular components of ex vivo gammadelta T cell expansions to optimize selection of potent cell therapy donors for neuroblastoma immunotherapy trials. *Oncoimmunology.* 2022;11(1):2057012.
58. Beltra JC, Bourbonnais S, Bédard N, Charpentier T, Boulangé M, Michaud E, et al. IL2R β -dependent signals drive terminal exhaustion and suppress memory development during chronic viral infection. *Proc Natl Acad Sci U S A.* 2016 Sep 13;113(37):E5444–53. doi:10.1073/pnas.1604256113.
59. Nishio N, Fujita M, Tanaka Y, Maki H, Zhang R, Hirose T, Demachi-Okamura A, Uemura Y, Taguchi O, Takahashi Y, et al. Zoledronate sensitizes neuroblastoma-derived tumor-initiating cells to cytolysis mediated by human $\gamma\delta$ T cells. *J Immunother.* 2012 Oct;35(8):598–606. doi:10.1097/CJI.0b013e31826a745a.